

Copyright WILEY-VCH Verlag GmbH & Co. KGaA, 69469 Weinheim, Germany, 2013.

# ADVANCED FUNCTIONAL MATERIALS

## Supporting Information

for *Adv. Funct. Mater.*, DOI: 10.1002/adfm.201202716

**Molten-Salt-Assisted Self-Assembly (MASA)-Synthesis of  
Mesoporous Metal Titanate-Titania, Metal Sulfide-Titania,  
and Metal Selenide-Titania Thin Films**

*Cüneyt Karakaya, Yurdanur Türker, and Ömer Dag\**

## Supporting Information

### Molten Salt Assisted Self-Assembly (MASA)-Synthesis of Mesoporous Metal Titanate-Titania, Metal Sulfide-Titania and Metal Selenide-Titania Thin Films

Cüneyt Karakaya, Yurdanur Türker, and Ömer Dag\*

Bilkent University, Department of Chemistry, 06800, Ankara, Turkey,  
[dag@fen.bilkent.edu.tr](mailto:dag@fen.bilkent.edu.tr)

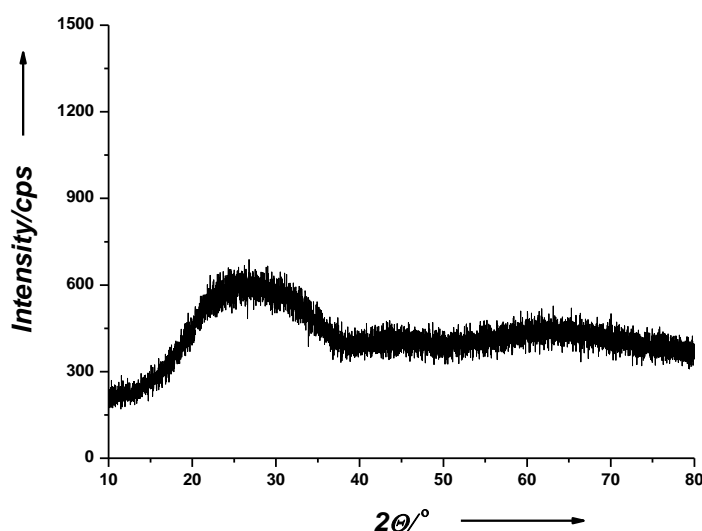


**Figure S1.** A representative XRD pattern of mesostructured  $[\text{Zn}(\text{H}_2\text{O})_6](\text{NO}_3)_2$ -Titania thin films.

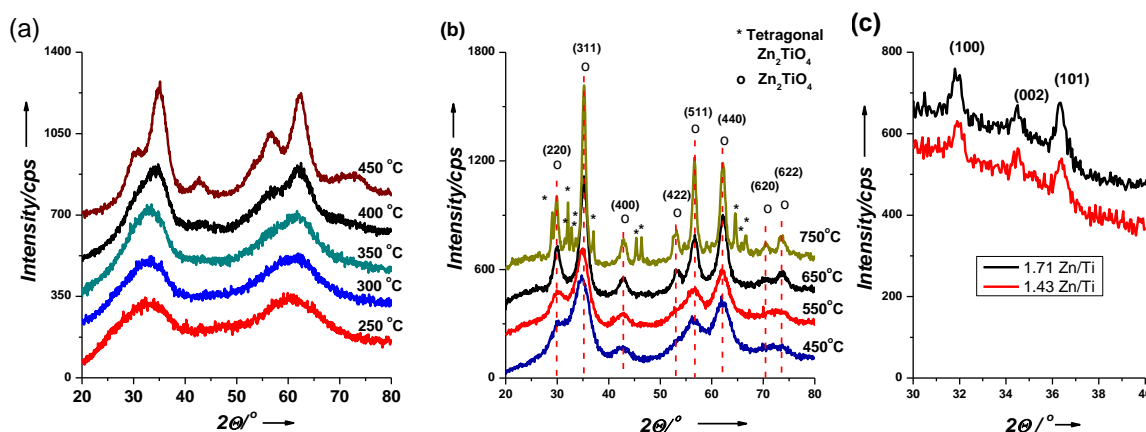


**Figure S2.** (a) XRD patterns of *meso*- $\text{Zn}_2\text{TiO}_4$  (with a Zn/Ti mole ratio of 0.86), annealed at 250, 300, 350, and 400 °C as marked on the patterns. (b) XRD patterns of *meso*- $\text{Zn}_2\text{TiO}_4$  (with a Zn/Ti mole ratio of 0.86), annealed at 450, 550, 650, and 750 °C as marked on the patterns. (c) XRD patterns of thin films with a Zn/Ti mole ratio of 1.43 and 1.71, calcined at 450 °C.

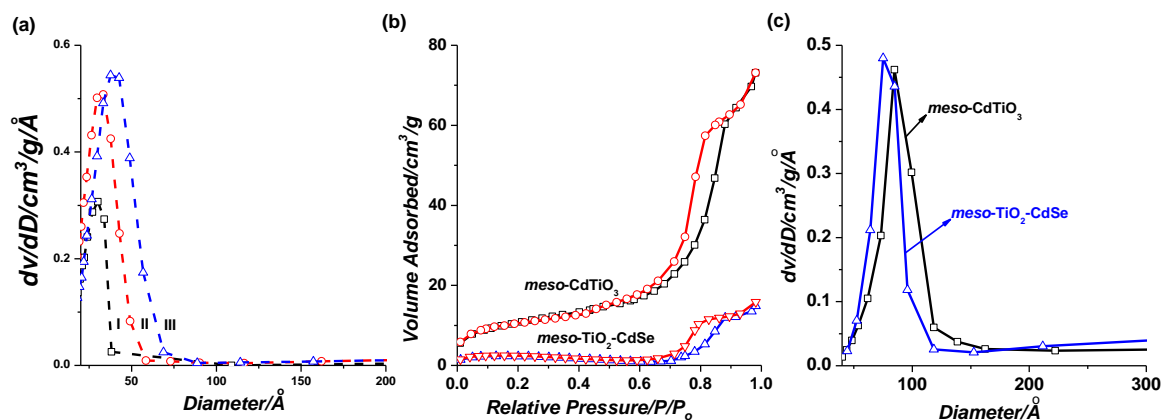


**Figure S3.** (a) Pore size distribution of  $\text{meso-Zn}_2\text{TiO}_4$  obtained from the samples in Figure 3(b) (the Zn/Ti mole ratios are (I) 0.29, (II) 0.57, and (III) 0.86). (b)  $\text{N}_2$ -sorption isotherms of  $\text{meso-CdTiO}_3$  and  $\text{meso-TiO}_2\text{-CdSe}$  and (c) pore size distribution plots of  $\text{meso-CdTiO}_3$  and  $\text{meso-TiO}_2\text{-CdSe}$  films,

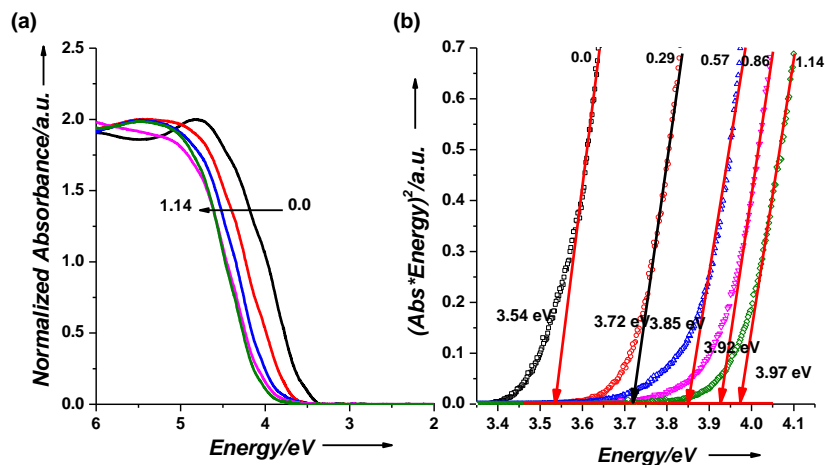


**Figure S4.** The normalized UV-Vis absorption spectra (a) and their plots (b) of  $\text{meso-Zn}_2\text{TiO}_4$  thin films with Zn(II)/Ti(IV) mole ratios of 0.29, 0.76, 0.86, and 1.14 (as labelled on the spectra).

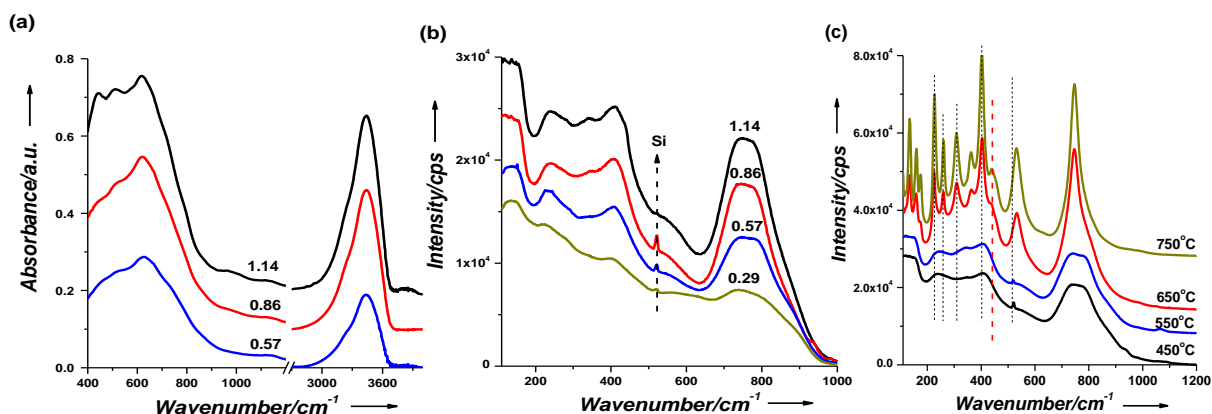


**Figure S5.** IR and Raman spectra of a set of *meso*-Zn<sub>2</sub>TiO<sub>4</sub> with different Zn/Ti mole ratios (as indicated on the spectra). (c) Raman spectra of *meso*-Zn<sub>2</sub>TiO<sub>4</sub>, annealed at 450, 550, 650, and 750 °C as marked on the patterns.

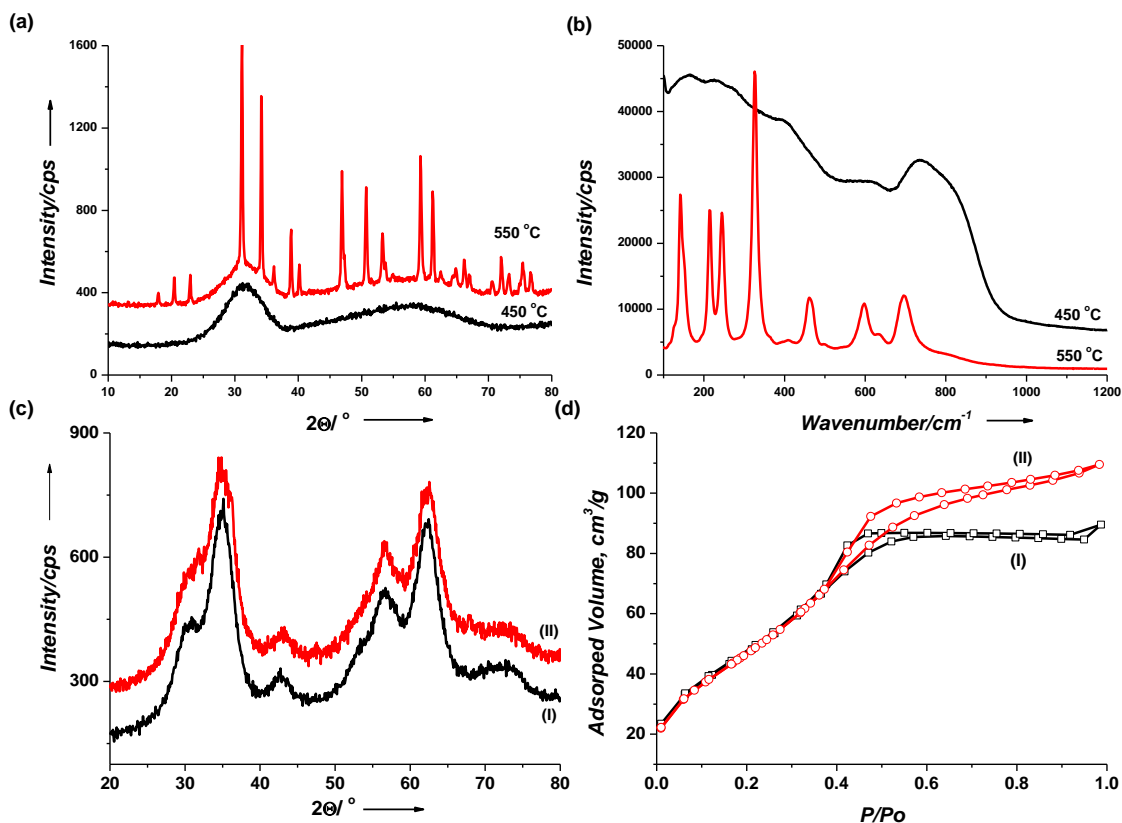


**Figure S6.** The spray coated samples: (a) The PXRD patterns of *meso*-CdTiO<sub>3</sub> at 450 °C and 550 °C. (b) The Raman spectra of *meso*-CdTiO<sub>3</sub> at 450 °C and 550 °C. (c) The PXRD patterns of (I) spray coated and (II) casted *meso*-Zn<sub>2</sub>TiO<sub>4</sub> with a Zn/Ti mole ratio of 0.86. (d) N<sub>2</sub>-sorption isotherms of (I) spray coated and (II) casted *meso*-Zn<sub>2</sub>TiO<sub>4</sub> with a Zn/Ti mole ratio of 0.86.

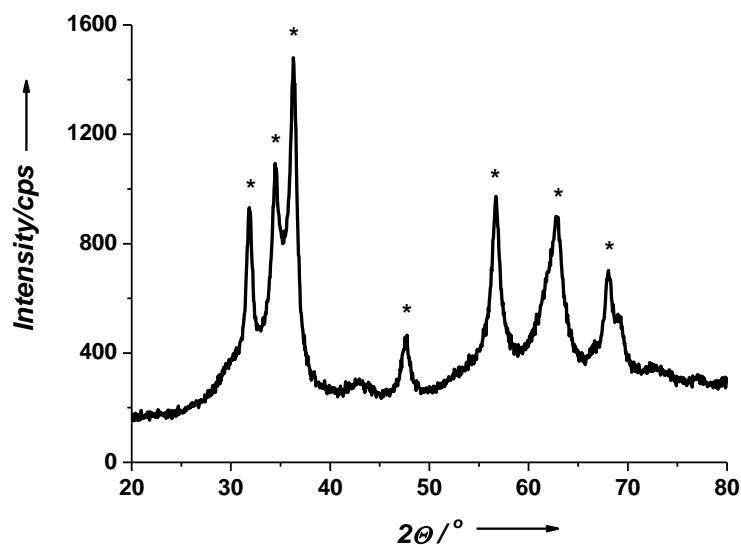


**Figure S7.** XRD pattern of SC film with Zn/Ti mole ratio of 1.71. The diffraction lines, marked asterisks, are due to wurtzite ZnO.

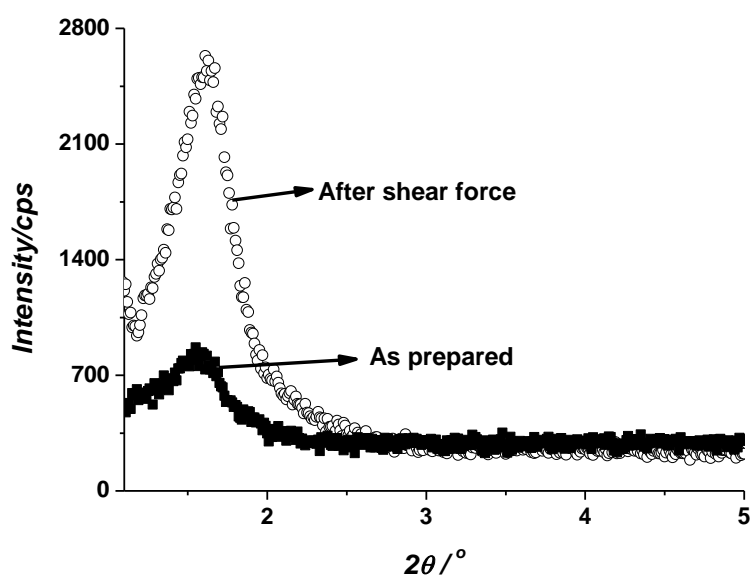


**Figure S8.** The XRD patterns of the spray coated films before and after shear force. The intensity of the XRD line increases 4-5 times, indicating orientation of the gel by shear force. This is a characteristic property of liquid crystals.

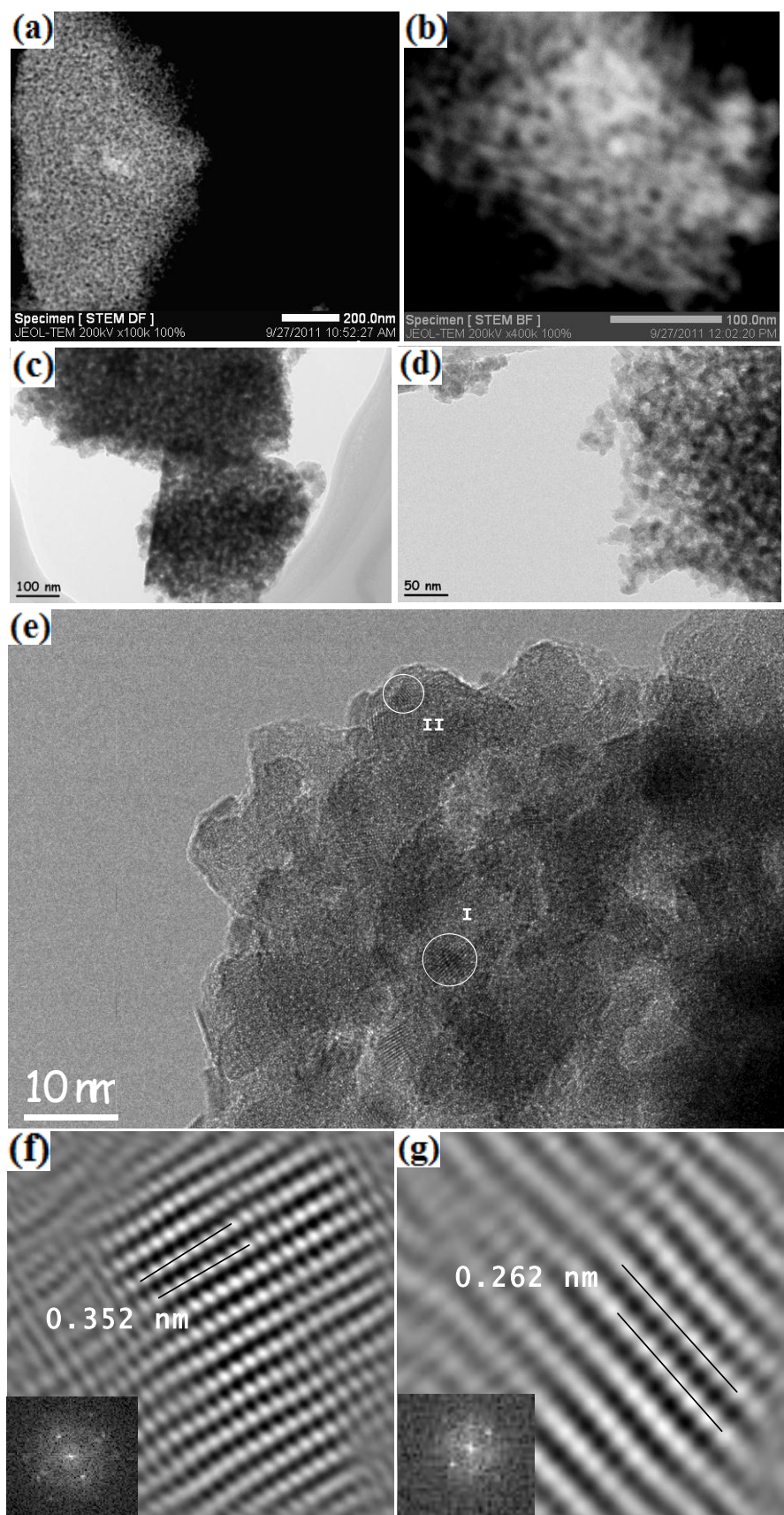


**Figure S9.** (a, b) Dark field and (c, d, and e) TEM images of meso-TiO<sub>2</sub>-CdSe at different magnifications, FFT (insets) and inverse FFT of the selected area I (f), and II (g) in panel (e).

XRD Pattern <sup>[1]</sup> of Zn <sub>2</sub> TiO <sub>4</sub> 2theta	XRD Pattern <sup>[1]</sup> of Zn <sub>2</sub> TiO <sub>4</sub> 2theta, (hkl)	Raman Peaks (cm <sup>-1</sup> )	XRD Pattern <sup>2</sup> of CdTiO <sub>3</sub> <sup>b</sup> 2theta, (hkl)	XRD Pattern <sup>[2]</sup> of CdTiO <sub>3</sub> <sup>b</sup> 2theta, (hkl)	Raman Peaks <sup>[3]</sup> (cm <sup>-1</sup> ) <sup>b</sup>
29.0	65.8	118 (sh)	17.9 (003)	59.3 (214)	127
30.6	66.7	134	20.4 (101)	61.2 (300)	142
31.5	68.7	159	23.0 (012)	62.5 (125)	150 (sh)
32.1		175	31.1 (104)	64.3 (303)	215
32.8	29.9 (220) <sup>a</sup>	225 <sup>a</sup>	34.2 (015)	64.8 (208)	245
33.6	35.2 (311) <sup>a</sup>	260 <sup>a</sup>	36.1 (113)	66.2 (1010)	326
37.0	42.9 (400) <sup>a</sup>	308 <sup>a</sup>	38.9 (021)	67.0 (119)	364 (sh)
45.3	52.8 (422) <sup>a</sup>	362 <sup>a</sup>	40.2 (021)	70.6 (217)	408
46.4	56.6 (511) <sup>a</sup>	403	46.8 (024)	72.0 (220)	462
53.2	62.1 (440) <sup>a</sup>	440	50.7 (116)	73.2 (306)	500 (sh)
54.7	70.5 (620) <sup>a</sup>	457 <sup>a</sup>	53.3 (018)	75.0 (223)	597
59.0	73.6 (622) <sup>a</sup>	530	54.0 (211)	75.4 (128)	633
60.0		747	54.8 (122)	76.7 (0210)	697
64.5		785			801(sh)

**Table S1.** The XRD Patterns and Raman Spectral Data of Zn<sub>2</sub>TiO<sub>4</sub> and CdTiO<sub>3</sub> (<sup>a</sup>Zn<sub>2</sub>TiO<sub>4</sub> (Cubic Phase), <sup>b</sup>Rhombohedral Phase of CdTiO<sub>3</sub>).

## References

- [1] ICDD PDF #00-025-1164 (Zn<sub>2</sub>TiO<sub>4</sub> Cubic Phase).  
[2] ICDD PDF #00-029-0277 (CdTiO<sub>3</sub> Rhombohedral Phase).  
[3] D. Bersani, P. P. Lottici, M. Canal, A. Montenero, G. Gnappi, *J. Sol Gel Sci. Tech.* **1997**, 8, 337.